HHS Public Access

Author manuscript

Mucosal Immunol. Author manuscript; available in PMC 2019 March 06.

Published in final edited form as:

Mucosal Immunol. 2018 November ; 11(6): 1582–1590. doi:10.1038/s41385-018-0066-8.

Natural killer T cells mediate inflammation in the bile ducts

N. L. Berntsen[1,2], **B. Fosby**[1,3], **C. Tan**[1], **H. M. Reims**[4], **J. Ogaard**[2], **X. Jiang**[1,2], **E. Schrumpf**[1,2], **L. Valestrand**[1,2], **T. H. Karlsen**[1,2,5,6], **P.-D. Line**[3,6], **R. S. Blumberg**[7], and **E. Melum**[1,2,5,6]

[1]Norwegian PSC Research Center, Department of Transplantation Medicine, Division of Surgery, Inflammatory Diseases and Transplantation, Oslo University Hospital Rikshospitalet, Oslo, Norway

[2]Research Institute of Internal Medicine, Division of Surgery, Inflammatory Diseases and Transplantation, Oslo University Hospital, Oslo, Norway

[3]Department of Transplantation Medicine, Division of Surgery, Inflammatory Diseases and Transplantation, Oslo University Hospital Rikshospitalet, Oslo, Norway

[4]Department of Pathology, Oslo University Hospital Rikshospitalet, Oslo, Norway

[5]Section for Gastroenterology, Department of Transplantation Medicine, Division of Surgery, Inflammatory Diseases and Transplantation, Oslo University Hospital Rikshospitalet, Oslo, Norway

[6]Institute of Clinical Medicine, Faculty of Medicine, University of Oslo, Oslo, Norway

[7]Division of Gastroenterology, Hepatology and Endoscopy, Department of Medicine, Brigham and Women's Hospital, Harvard Medical School, Boston, MA 02115, USA

Abstract

Cholangiocytes function as antigen-presenting cells with CD1d-dependent activation of natural killer T (NKT) cells in vitro. NKT cells may act both pro- and anti-inflammatory in liver immunopathology. We explored this immune pathway and the antigen-presenting potential of NKT cells in the bile ducts by challenging wild-type and *Cd1d*$^{-/-}$ mice with intrabiliary injection of the NKT cell activating agent oxazolone. Pharmacological blocking of CD1d-mediated activation was performed with a monoclonal antibody. Intrabiliary oxazolone injection in wild-type mice caused acute cholangitis with significant weight loss, elevated serum levels of alanine

Correspondence: E Melum (espen.melum@medisin.uio.no).

AUTHOR CONTRIBUTIONS

N.L.B.: study concept and design, acquisition of data, statistical analysis and interpretation of data and drafting of the manuscript. C.T., L.V. and J.O.: acquisition of data, technical support and critical revision of the manuscript for important intellectual content. B.F., X.J. and E.S.: study concept and design and critical revision of the manuscript for important intellectual content. H.M.R., T.H.K. and P.-D.L.: study concept and design and critical revision of the manuscript for important intellectual content. R.S.B.: study concept and design, interpretation of data and critical revision of the manuscript for important intellectual content. E.M.: study concept and design, analysis and interpretation of data, drafting of the manuscript, critical revision of the manuscript for important intellectual content, obtained funding and study supervision.

ADDITIONAL INFORMATION

The online version of this article (https://doi.org/10.1038/s41385-018-0066-8) contains supplementary material, which is available to authorized users.

Competing interests: The authors declare no competing interests.

transaminase, aspartate transaminase, alkaline phosphatase and bilirubin, increased histologic grade of cholangitis and number of T cells, macrophages, neutrophils and myofibroblasts per portal tract after 7 days. NKT cells were activated after intrabiliary injection of oxazolone with upregulation of activation markers. *Cd1d*$^{-/-}$ and wild-type mice pretreated with antibody blocking of CD1d were protected from disease. These findings implicate that cells in the bile ducts function as antigen-presenting cells in vivo and activate NKT cells in a CD1d-restricted manner. The elucidation of this biliary immune pathway opens up for potentially new therapeutic approaches for cholangiopathies.

INTRODUCTION

Cholangiopathies such as primary sclerosing cholangitis (PSC) and primary biliary cholangitis (PBC) target the bile ducts and cause major liver-related morbidity and mortality due to a progressive disease course.[1–3] The etiology and pathophysiology remain largely elusive for these conditions, with the concurring challenge of limited treatment options and consequential cirrhosis and liver failure requiring liver transplantation.[1–3] PSC and PBC are complex immune-mediated diseases where genetic risk loci suggest an involvement of the immune system, which is further supported by functional studies.[3–6] The biliary anatomy limits the accessibility to the bile ducts in experimental models and complicates the study of biliary immunopathology.

The biliary epithelium is an active participant in biliary inflammation and fibrogenesis,[7,8] in addition to its main biological responsibility of bile secretion and composition modification. Cholangiocytes constitutively express major histocompatibility complex (MHC) class I molecules,[9] while MHC class II expression is induced or upregulated in certain disorders such as PBC,[10] PSC[11] and biliary atresia.[12] In spite of MHC expression, it has been difficult to demonstrate that cholangiocytes can function as antigen-presenting cells (APCs) with presentation of peptide antigens,[8,13–15] but in vitro studies have demonstrated activation of unconventional T lymphocyte subsets such as natural killer T (NKT) and mucosal-associated invariant T (MAIT) cells through presentation of lipid or bacterial-derived small molecular antigens dependent on the MHC class I-related molecules CD1d or MR1, respectively.[16,17] This may be of importance in biliary pathophysiology as the cells in the bile ducts are continuously exposed to potential antigens in bile, which is rich in lipids and may contain bacterial components, particularly in cholangiopathies.[18–20]

NKT cells are classified as type I or II dependent on the composition of their T cell receptor (TCR) and antigen specificity.[21] Type I, also known as invariant NKT (iNKT) cells, express a semiinvariant TCR and are characterized by their alpha-galactosylceramide (α-GalCer)-ligand specificity, while type II display a more diverse TCR repertoire, respond to other glycolipids and represent less than 5% of hepatic NKT cells in mice.[21–23] NKT cells are abundant in liver and highly conserved in mammals.[23–26] Taken together with a widespread tissue distribution of CD1d, this points to a crucial importance of NKT cells in different immune functions.[27,28] They can rapidly produce Th1 (e.g., interferon-γ (IFN-γ), tumor necrosis factor), Th2 (e.g., interleukin (IL)-4, IL-13) and Th17 (e.g., IL-17, IL-22) cytokines upon activation[21,23] and act as immunoregulators with either protective or pathogenic effects

in response to microorganisms[29] in autoimmune disorders,[30] allergy,[31] cancer or tumor surveillance.[32] Animal models such as concanavalin A- and α-GalCer-induced liver injury mimicking autoimmune hepatitis suggest that NKT cells may have both pro- and anti-inflammatory roles in autoimmune liver disease, mediated through IL-4 or IL-17, respectively.[33,34] Previous observations of changes in NKT cell numbers in certain liver disorders (e.g., PBC[35]), variation of CD1d expression with disease severity[16,36] and inhibition of viral hepatitis B replication[37,38] point to a potentially important role of this immune pathway in liver and biliary immunopathology. Furthermore, microbial-derived CD1d-restricted lipid antigens have been shown to be crucial for NKT cell-dependent development of liver autoimmunity and PBC-like disease with signature antibodies in mice.[39]

We hypothesized that CD1d-dependent activation of NKT cells represents an important immunoregulatory pathway in the bile ducts. To explore this, we used a model based on intrabiliary injection of oxazolone, a sensitizing agent commonly used to study NKT cell-mediated inflammation and hapten-mediated inflammatory disorders of the skin and colon.[40–42]

RESULTS

Oxazolone injection in the bile ducts causes liver disease

To investigate whether NKT cells could be activated in the bile ducts we performed skin presensitization followed by intrabiliary re-challenge with oxazolone, which is known to activate NKT cells, in wild-type (WT) mice and compared with injection of vehicle control (Fig. 1a, Supplementary Fig. 1). No peri- or immediate postoperative (<24 h) mortality was observed, which indicates that mice tolerate the surgery well (Fig. 1b). As expected after major surgery, we observed an initial weight loss in all mice that peaked 2 days after surgery, with a complete regain of the starting weight by day 6 in the vehicle group, while the oxazolone group did not regain their starting weight (Fig. 1c). At day 2, the mice in the oxazolone group suffered significantly larger weight loss, as well as increased pain and reduced activity, compared with the vehicle controls (Fig. 1c, d). Alanine transaminase (ALT) serum levels also peaked with a nonsignificant increase in the oxazolone group compared with the vehicle controls at day 2 after surgery and were significantly higher at the time of killing (Fig. 1e and data not shown). In line with the ALT results, aspartate transaminase (AST), alkaline phosphatase (ALP) and bilirubin had a nonsignificant increase when comparing oxazolone with vehicle on day 2 after surgery with clear difference at the time of killing (Fig. 1f, h). There were no significant differences in total weight or weight adjusted for the total body weight of neither liver nor spleen when comparing oxazolone with vehicle (data not shown).

To test the effects of directly exposing the biliary epithelium to other known NKT cell activating antigens we compared bile duct injection of α-GalCer to the already established model of intraperitoneal (i.p.) α-GalCer injection.[43] Biliary injection of α-GalCer mimicked the effects of i.p. injection with comparable rise in ALT levels and increase in serum concentrations of IL-4 and IFN-γ, indicating NKT cell activation and similar

histopathological changes in the liver with a nonsignificant increase in portal inflammation (data not shown).

Oxazolone injection in the bile ducts leads to inflammation in the portal area

Next, we evaluated whether the deteriorated clinical condition after intrabiliary injection of oxazolone in mice was paralleled by histopathological changes in the liver. The grade of cholangitis (based on observed portal inflammation and necrosis) showed that oxazolone cause significant pathology compared with vehicle at both day 2 after surgery and at the time of killing, which was also clear from macroscopic examination of the livers (Fig. 2a, b). The histological grade of portal inflammation was significantly higher in the oxazolone group compared to vehicle (1.2 vs. 0.5, $P = 0.005$, oxazolone vs. vehicle respectively) with significant increases in infiltration of CD3-, Ly6G- and Mac-2-positive inflammatory cells (Fig. 2c). Quantitative image analysis comparing paired immunohistochemical detection of CD1d and CK19 showed no significant difference in CD1d expression on the biliary epithelium at 7 days after intrabiliary injection of oxazolone or vehicle (Supplementary Fig. 2).

Oxazolone causes development of fibrosis

Within 7 days after surgery, we observed that oxazolone injection also causes fibrotic changes in the liver with significantly higher number of α-SMA$^+$ cells surrounding the bile ducts (Fig. 2d) and differences in the relative expression of fibrosis marker genes, with a significant increase in *Timp1,* as well as increased expression of *Col3a1, Col1a1* and *Mmp2* (Fig. 2e, Supplementary Fig. 3A-C). The microscopic grade of peribiliary fibrosis (1.1 vs. 0.5, $P = 0.09$, when comparing oxazolone to vehicle, respectively) and collagen production visualized by Sirius red staining was non-significantly increased (Supplementary Fig. 3D-E).

Chronic effects of oxazolone cholangitis

To evaluate the long-term effects of oxazolone cholangitis we subjected mice to intrabiliary oxazolone injection and followed them for 6 or 12 weeks before killing. The mice were weighed daily or every second day for the first week, then twice a week from the second week until killing. Serum samples for ALT measurements were collected once a week. We confirmed previous observations of more severe disease in mice injected with oxazolone, as signified by larger weight loss that occasionally culminated in death when comparing oxazolone with vehicle control (Fig. 3a and data not shown) and significantly higher serum ALT levels 1 and 2 weeks after surgery (Fig. 3b). There were no significant differences in serum ALT levels from 3 to 6 or 12 weeks after surgery, nor in serum AST, ALP or bilirubin after 6 weeks (Fig. 3b and data not shown). Compared to the inflammatory changes observed after 1 week, there were less severe histopathological changes in the long-term experiments with a trend to continued increased portal inflammation after 6 weeks ($P = 0.07$) and increased number of CD3-positive cells (data not shown and Fig. 3c). The mice injected with oxazolone had significantly increased microscopic grade of peribiliary fibrosis after both 6 and 12 weeks compared with vehicle control, but no difference in the number of α-SMA$^+$ cells surrounding the bile ducts (Fig. 3d, e and data not shown).

Oxazolone injection in the bile ducts leads to activation of iNKT cells

To determine whether injection of oxazolone into the bile ducts would cause activation of NKT and the remaining T cells (i.e., CD1d tetramer negative), we extracted liver and spleen lymphocytes from mice 2 days after intrabiliary injection with either oxazolone or vehicle. We observed clear activation of liver invariant NKT (iNKT) cells with significantly increased expression of activation marker CD69 and a nonsignificant increase in CD25 (Fig. 4), as well as a tendency for increased activation of both markers in spleen iNKT cells (Supplementary Fig. 4A) when comparing oxazolone with vehicle. There was a nonsignificant activation of CD1d tetramer-negative T cells in spleen and liver when comparing intrabiliary injection of oxazolone with vehicle, as demonstrated by a nonsignificant increase of CD25 and of both CD25 and CD69 in spleen and liver tetramer-negative T cells respectively (Supplementary Fig. 4). We did not see any significant differences in the iNKT cell fraction of lymphocytes in neither liver nor spleen (data not shown).

Oxazolone cholangitis is dependent upon CD1d and NKT cells

To examine whether the biliary inflammation induced by oxazolone was NKT cell dependent, we challenged *Cd1d*$^{-/-}$ and WT mice with intrabiliary oxazolone. *Cd1d*$^{-/-}$ mice appeared to be protected from disease with significantly better survival compared with WT mice (Fig. 5a). There was a significant increase in production of IFN-γ and IL-4 in WT mice (Fig. 5b) and WT mice suffered more severe liver inflammation with significantly higher weight loss (Fig. 5c) and peak ALT serum levels 2 days after surgery (Fig. 5d), as well as a tendency for increased portal inflammation 7 days after surgery (Fig. 5e, f).

We next aimed to investigate whether pharmacological blocking of CD1d could prevent the pathology caused by oxazolone and subjected WT mice to the intrabiliary injection of oxazolone as before but with i.p. injection of a CD1d-blocking antibody, 19G11, at two time points: first at the time of skin sensitization and second the day before the surgery and compared with injection of an isotype control antibody (Fig. 5g). Mice injected with 19G11 were protected from disease with increased survival (Fig. 5h) and improved disease parameters, i.e., significantly less weight loss (Fig. 5i) and lower peak serum ALT levels (Fig. 5j). High mortality in mice injected with isotype control antibody precluded histology scoring and immunohistochemical staining in these experiments.

Intrabiliary injection of oxazolone does not cause inflammation of the bowel

As some of the intrabiliary injected fluid eventually will enter the bowel following release of the common bile duct clamp, we performed a histopathological evaluation of duodenal, ilieal and colonic segments. We did not observe any signs of epithelial injury or inflammation in either gut segments (Supplementary Fig. 5).

DISCUSSION

In the present study we show that injection of an exogenous compound known to activate NKT cells, oxazolone, leads to cholangitis that is CD1d dependent. Our findings implicate that cells in the bile ducts function as APCs in vivo and activate NKT cells in a CD1d-

restricted manner. The elucidation of this pathway for immune activation in the biliary tree opens up for potentially new therapeutic approaches.

Cholangiocytes express both classical antigen-presenting molecules such as MHC class I and II and the MHC homologs CD1d and MR1.[9,10,16,17] In vitro assays have demonstrated that cholangiocytes function as APCs and present both endogenous and exogenous lipid and microbial-derived antigens to NKT and MAIT cells, but it is still unclear if they can also present peptide antigens and activate classical MHC-restricted T cells.[13,15–17] We aimed to study the role of immune activation in the bile ducts in vivo and hypothesized that CD1d-mediated inflammation is of importance in the bile ducts, where cholangiocytes are the predominant cell type. The anatomy of the biliary tree complicates access to the bile ducts for in vivo immunological studies. We injected oxazolone into the bile ducts by applying a bile duct injection technique (Supplementary Fig. 1). One of the advantages to this surgical model is that it directly exposes cells in the bile duct to antigens. We compared bile duct injection of α-GalCer to the already established model of i.p. α-GalCer injection[43] and found that bile duct injection of α-GalCer mimicked the effects of i. p. injection. Lipid antigens may be loaded onto CD1 molecules during assembly in the endoplasmic reticulum, directly on the cell surface or in different intracellular compartments after cell uptake and processing of exogenous lipids.[44,45] We have demonstrated in a previous study that CD1d expression on cholangiocytes seems to be predominately basolateral, which suggests that they may parallel intestinal epithelial cells with a more efficient basolateral antigen presentation.[16,46] This is supported by our observation of basolateral infiltration of inflammatory cells that surround the bile ducts that suggests apical antigen uptake and subsequent basolateral presentation, although we cannot rule out other mechanisms of antigen distribution.

Injection of oxazolone in the bile ducts mimics the oxazolone colitis model characterized by a rapid onset of inflammation that peaks by day 2 and either quickly resolves or causes death of the mouse.[40] Biliary oxazolone injection appears to be primarily a model of acute inflammation with a rapid disease onset expressed through significant weight loss, decreased activity, rise in serum liver disease markers such as ALT, AST, ALP and bilirubin and histological injury such as portal necrosis and infiltration of inflammatory cells within 2 days after surgery. Long-term experiments showed resolution of inflammation, relatively quick weight recovery and reduction of serum liver disease markers, but sustained portal fibrosis. One of the challenges in establishing the oxazolone cholangitis model was to find a solvent for oxazolone that did not cause damage to the bile ducts or surrounding liver tissue. While the surgery and bile duct injection do not cause any tissue damage in itself, the need to use 65% dimethyl sulfoxide (DMSO) to achieve a concentration of 1% oxazolone means that we need to accept some minor injury in the vehicle group (e.g., small bile infarcts likely due to toxicity of DMSO in high concentrations). The observation that increased serum biliary disease markers coincided with enhanced serum ALT and AST levels may be explained by the co-occurring development of portal inflammation and likely exposure of bile acids to the hepatocytes. Serum elevation of ALT and AST is also frequently observed in PBC and PSC as well as in multiple mouse models of cholangiopathies. Another limitation of the model is leakage of oxazolone into the intestines with the risk of causing gut inflammation after release of the common bile duct clamp. To address this, we

systematically investigated duodenal, ileal and colonic gut segments and did not see any signs of epithelial injury or inflammation.

We observed an increased level of CD3-positive cells in mice injected with oxazolone and given the frequency of hepatic NKT cells in mice a large proportion of these were likely NKT cells.[24,25] The NKT cells in livers from mice injected with oxazolone had an activated phenotype pointing to a crucial role of NKT cells in this model. The nonsignificant activation of spleen NKT cells after oxazolone injection suggests involvement of systemic immune effects, which is supported by increased weight loss and a nonsignificant increase in activation markers of tetramer-negative T cells. NKT cell activation initiates cross talk with other immune cells[21] and we observed significant increase of peribiliary CD3-, Ly6G- and Mac-2-positive inflammatory cells after injection of oxazolone in the bile ducts, indicating that lymphocytes, neutrophils and macrophages contribute to the inflammation.

By using *Cd1d*$^{-/-}$ mice we demonstrated that NKT cells are important in driving oxazolone cholangitis, but the observation of some residual disease in the *Cd1d*$^{-/-}$ mice indicates that other pathways are also of importance. To further demonstrate that activation of NKT cells is dependent on CD1d-mediated antigen presentation and not through other CD1d-independent cytokine-driven pathways (e.g., IL-12 and IL-18), we pharmacologically blocked CD1d antigen presentation and demonstrated that these mice were also protected from disease. The acute onset of disease with rapid resolution of morphological changes and disease parameters, as demonstrated by rapid recovery and only some sustained fibrosis in long-term-experiments, complicates measurement of treatment effects of therapeutic efforts made after development of significant disease.

Human liver diseases such as PBC, PSC and autoimmune hepatitis are associated with gut inflammation;the strongest link being between inflammatory bowel disease and PSC.[7] As the bile ducts are continuous with the intestinal lumen, the cholangiocytes are exposed to potential lipid and microbial-derived antigens from both gut and liver.[16,17,20] NKT cells are important contributors in host defense against various pathogens, but how they may interact with commensal bacteria is currently unknown.[47] Animal models suggest that NKT cells may have both protective and detrimental roles in liver disease, as for inflammatory bowel disease.[33,34,37,42] CD1d crosslinking on intestinal epithelial cells seems to protect against inflammation in oxazolone-induced colitis mediated by NKT cells through IL-10 production.[48] While downregulation of CD1d on the biliary epithelium in advanced liver disease suggests a potential role of NKT cells in disease pathogenesis, the nature of this involvement and the significance of CD1d expression on cholangiocytes remains to be understood.[16] There was no significant difference in CD1d expression on the biliary epithelium 7 days after intrabiliary injection of oxazolone or vehicle.

In conclusion, we have demonstrated that CD1d-mediated activation of NKT cells in the bile ducts may lead to cholangitis in which cells in the bile ducts likely act as APCs. As the cholangiocytes are not only a disease target in cholangiopathies, but also active participants in bile duct inflammation, further studies on their role in maintaining homeostasis and interplay with the immune system may help to better understand the pathoetiologies of often detrimental biliary disorders such as PSC and PBC and thereby guide future therapy.[1,3,7]

Our results suggest that modulation of immune pathways involving NKT cells can represent a novel therapeutic approach in liver and biliary disorders.

METHODS

Mice

Specific pathogen-free male and female C57BL/6 WT mice (The Jackson Laboratory, Bar Harbor, ME, USA) and previously described CD1d-deficient mice (*Cd1d*$^{-/-}$) on a C57Bl/6 background[49] were housed in a Minimal Disease Unit at the animal facility at Oslo University Hospital Rikshospitalet, Oslo, Norway, with a 12-h light-dark cycle and ad libitum access to water and standard rodent diet. All experiments were performed with co-housed age- and sex-matched mice and with littermate controls for all experiments comparing *Cd1d*$^{-/-}$ and WT mice. Mice undergoing surgery were not fasted and were of 9–10 weeks of age at the time of surgery, which was carried out during the light cycle.

All animals received humane care and the animal experiments were approved by the Norwegian National Animal Research Authority (project license no FOTS 5279) and performed in accordance with the European Directive 2010/63/EU, the Animal Research: Reporting of In Vivo Experiments guidelines and The Guide for the Care and Use of Laboratory Animals, 8th edition (NRC 2011, National Academic Press).

Oxazolone presensitization

We performed presensitization as described previously with application of 200 μl 3% oxazolone (4-ethoxymethylene-2-phenyl-2-oxazoline-5-one, Sigma Aldrich, St. Louis, MO, USA) dissolved in 100% ethanol to the pre-shaved skin of the mouse abdomen 5 days prior to surgery.[42]

The bile duct injection technique

All procedures were performed using proper analgesia and general anesthesia with either isoflurane gas or i.p. injection with FD2 (Fentanyl/Domitor/Dormicum) and Antisedan (antagonist) post surgery. We performed injection into the biliary tree according to a bile duct injection technique recently established[50] (Supplementary Fig. 1). In brief, we performed a median laparotomy, clamped the common bile duct before it meets with the pancreatic duct to temporarily obstruct bile flow and to prevent any injected fluid from entering the duodenum directly without going into the liver. The gall bladder was catheterized and 1 μl/g total body weight of fluid was slowly injected with the aid of a 100 μl fine precision syringe (Hamilton Company, Bonaduz, Switzerland) into the bile ducts through the catheter, at a maximum speed of 1 μl/s. We injected either 1% oxazolone dissolved in 65% DMSO mixed with phosphate-buffered saline (PBS) or 65% DMSO as a vehicle control. The injected fluid was colored blue with a Patent Blue V, sodium salt (Acros Organics, Fischer Scientific, MA, USA) to visualize fluid entry into the biliary tree. After injecting, the clamp was removed from the common bile duct that was confirmed still patent by the flow of blue-colored bile into the duodenum and the catheter was removed by gentle retraction while performing a functional cholecystectomy.

Intraperitoneal antibody injections.

WT mice were injected i.p. with 500 μg of an anti-CD1d-blocking antibody (19G11, BioXCell, West Lebanon, NH, USA) or an isotype control (LTF-2, BioXCell) in sterile PBS at two time points: first on the day of the presensitization and second the day prior to surgery.

Mouse monitoring, tissue collection and extraction of primary lymphocytes

All mice were monitored as indicated with observation of the clinical state, registration of total body weight and pain and with blood collection from the saphenous vein. Mice were killed and body, liver and spleen weights were recorded. Blood, liver and gut tissue was collected and extraction of primary lymphocytes from spleen and perfused livers was performed. See Supplementary Methods for further details.

Biochemistry

ALT was measured in serum applying an ALT/SGBT Liqui-UV® test reagent kit (Stanbio Laboratory, TX, USA) or using an ADVIA 1800 (Siemens, Munich, Germany) at The Central Laboratory, Norwegian School of Veterinary Science, together with serum measurements of AST, bilirubin and ALP. IL-4 and IFN-γ were measured in serum with Mouse IL-4 and Mouse IFN-γ ELISA Sets (BD Biosciences).

Flow cytometry

Primary lymphocytes in single-cell suspensions were incubated with Fc-block (anti-mouse CD16/32, clone 93, BioLegend, San Diego, CA, USA) to avoid non-specific binding. Lymphocytes were stained for 1 h with PE-labeled α-GalCer-loaded PBS-57 CD1d tetramers (kindly provided by the NIH Tetramer Core, Emory, GA, USA) and monoclonal antibodies (detailed antibody information is provided in (Supplementary Table 1). Flow cytometric analysis was performed using a BD FACSVerseTM flow cytometer (BD Biosciences) and results were analyzed in FlowJo version 9.5.4 (TreeStar, Ashland, OR, USA).

Histology and scoring

The liver and gut tissue were fixed, paraffin embedded, cut, deparaffinized, stained with hematoxylin and eosin (H&E) or Sirius red and evaluated in a blinded fashion (Supplementary Fig. 6). See the Supplementary Methods for further details.

Immunohistochemistry.

Immunohistochemical staining of CD3, Mac-2, lymphocyte antigen 6 complex locus G6D (Ly6G) and α-smooth muscle actin (α-SMA) was performed as described in the Supplementary Methods. Detailed antibody information is provided in Supplementary Table 1. For quantification, CD3-, α-SMA-, Ly6G- and Mac-2-positive cells located by the bile ducts were manually counted in six different 40× high-power fields on each slide in a blinded fashion, and the mean positive count was used in further analysis. Further details are included in the Supplementary Material.

Immunofluorescence, quantification of CD1d expression and image processing.

Sections of cryopreserved liver tissue were co-stained with anti-CD1d and anti-CK19 antibodies and mounted with 4′,6-diamidino-2-phenylindole (DAPI;Invitrogen, Thermo Fisher Scientific). All CD1d/CK19/DAPI-stained sections were scanned, digitized and analyzed semi-automatically in a blinded fashion. The CK19-positive cells were used to define the areas for quantification and the mean value of CD1d expression from >4 individual CK19-positive stained regions in each slide was used in further analysis. Images were acquired with identical exposure times and camera settings. Further details are included in the Supplementary Material.

RNA isolation, reverse transcription and quantitative real-time PCR Total RNA from RNAlater-stabilized liver tissue was isolated, and reverse transcription and quantitative real-time PCR were performed as described in the Supplementary Methods. Primers for the following genes were used: *collagen 3a1* (*Col3a1*), *collagen 1a1* (*Col1a1*), *matrix metalloproteinase 2* (*Mmp2*) and *tissue inhibitor of metalloproteinases 1* (*Timp1*), while *beta-actin* (*Actb*) or *glyceraldehyde 3-phosphate dehydrogenase (Gapdh)* were used as reference genes. Detailed primer information is provided in Supplementary Table 2. The relative expression of each sample was first normalized to the reference gene expression (*Actb* or *Gapdh*), then normalized to the average expression in samples from control mice and further analyzed according to the $2^{-\Delta\Delta CT}$ method.

Statistical analysis

Unless stated otherwise all values are presented as means ± SEM. To compare results for statistical significance we applied unpaired Student's *t*-test for variables meeting requirements of normal distribution and Mann–Whitney *U* test for variables not meeting the requirements for normal distribution. We visualized survival using Kaplan–Meier curves for survival from the time of surgery and the log-rank test was used to compare groups. We used GraphPad Prism version 6.0 (GraphPad Software, La Jolla, CA, USA) for all statistical analysie. *P* values lower than 0.05 were considered statistically significant.

Supplementary Material

Refer to Web version on PubMed Central for supplementary material.

ACKNOWLEDGEMENTS

The authors wish to thank Anne Pharo, Lisa Yuen Løvold, Liv Wenche Thorbjørnsen, Tonje Bjørnetrø, Hege Dahlen Sollid and Eva Kristine Klemsdal Henriksen at the Norwegian PSC Research Center, as well as Ellen Hellesylt at Laboratory of Immunohistochemistry, Department of Pathology, Radiumhospitalet, for great assistance and technical help. Loaded and unloaded PBS-57 CD1d tetramers were kindly provided by the NIH Tetramer Core, Emory, GA, USA. The study was supported by South Eastern Norway Regional Health Authority (project number 2013020), PSC Partners Seeking a Cure and the Norwegian PSC Research Center. R.S.B. was supported by NIH DK44319.

REFERENCES

1. Lazaridis KN & Larusso NF. The cholangiopathies. Mayo Clin. Proc. 90, 791–800 (2015). [PubMed: 25957621]

2. Hirschfield GM, Karlsen TH, Lindor KD & Adams DH Primary sclerosing cholangitis. Lancet 382, 1587–1599 (2013). [PubMed: 23810223]

3. Hirschfield GM & Gershwin ME The immunobiology and pathophysiology of primary biliary cirrhosis. Annu. Rev. Pathol. Mech. Dis. 8, 303–330 (2013).

4. Yoshida K et al. Deletion of interleukin-12p40 suppresses autoimmune cholangitis in dominant negative transforming growth factor β receptor type II mice. Hepatology 50, 1494–1500 (2009). [PubMed: 19676134]

5. Maroni L et al. Knockout of the primary sclerosing cholangitis-risk gene Fut2 causes liver disease in mice. Hepatology 66, 542–554 (2017). [PubMed: 28056490]

6. Jiang X & Karlsen TH Genetics of primary sclerosing cholangitis and pathophysiological implications. Nat. Rev. Gastroenterol. Hepatol. 14, 279–295 (2017). [PubMed: 28293027]

7. Trivedi PJ & Adams DH Mucosal immunity in liver autoimmunity: a comprehensive review. J. Autoimmun. 46, 97–111 (2013). [PubMed: 23891169]

8. Kamihira T et al. Biliary epithelial cells regulate autoreactive T cells: implications for biliary-specific diseases. Hepatology 41, 151–159 (2005). [PubMed: 15619239]

9. Barbatis C et al. Immunohistochemical analysis of HLA (A, B, C) antigens in liver disease using a monoclonal antibody. Gut 22, 985–991 (1981). [PubMed: 7033057]

10. Ballardini G et al. Aberrant expression of HLA-DR antigens on bileduct epithelium in primary biliary cirrhosis: relevance to pathogenesis. Lancet 324, 1009–1013 (1984).

11. Chapman RW, Kelly PM, Heryet A, Jewell DP & Fleming KA Expression of HLA-DR antigens on bile duct epithelium in primary sclerosing cholangitis. Gut 29, 422–427 (1988). [PubMed: 3286382]

12. Feng J, Li M, Gu W, Tang H & Yu S The aberrant expression of HLA-DR in intrahepatic bile ducts in patients with biliary atresia: an immunohistochemistry and immune electron microscopy study. J. Pediatr. Surg. 39, 1658–1662 (2004). [PubMed: 15547830]

13. Leon MP et al. Immunogenicity of biliary epithelium: investigation of antigen presentation to CD4+ T cells. Hepatology 24, 561–567 (1996). [PubMed: 8781325]

14. Kamihira T et al. Distinct costimulation dependent and independent auto-reactive T-cell clones in primary biliary cirrhosis. Gastroenterology 125, 1379–1387 (2003). [PubMed: 14598254]

15. Barnes BH et al. Cholangiocytes as immune modulators in rotavirus-induced murine biliary atresia. Liver Int. 29, 1253–1261 (2009). [PubMed: 19040538]

16. Schrumpf E et al. The biliary epithelium presents antigens to and activates natural killer T cells. Hepatology 62, 1249–1259 (2015). [PubMed: 25855031]

17. Jeffery HC et al. Biliary epithelium and liver B cells exposed to bacteria activate intrahepatic MAIT cells through MR1. J. Hepatol. 64, 1118–1127 (2016). [PubMed: 26743076]

18. Olsson R et al. Bile duct bacterial isolates in primary sclerosing cholangitis: a study of explanted livers. J. Hepatol. 28, 426–432 (1998). [PubMed: 9551680]

19. Hiramatsu K et al. Amplification and sequence analysis of partial bacterial 16S ribosomal RNA gene in gallbladder bile from patients with primary biliary cirrhosis. J. Hepatol. 33, 9–18 (2000). [PubMed: 10905580]

20. Arrese M & Trauner M Molecular aspects of bile formation and cholestasis. Trends Mol. Med. 9, 558–564 (2003). [PubMed: 14659471]

21. Brennan PJ, Brigl M & Brenner MB Invariant natural killer T cells: an innate activation scheme linked to diverse effector functions. Nat. Rev. Immunol. 13, 101–117 (2013). [PubMed: 23334244]

22. Kawano T et al. CD1d-restricted and TCR-mediated activation of Va14 NKT cells by glycosylceramides. Science 278, 1626–1629 (1997). [PubMed: 9374463]

23. Santodomingo-Garzon T & Swain MG Role of NKT cells in autoimmune liver disease. Autoimmun. Rev. 10, 1–8 (2011).

24. Eberl G et al. Tissue-specific segregation of CD1d-dependent and CD1d-independent NKT cells. J. Immunol. 162, 6410–6419 (1999). [PubMed: 10352254]

25. Matsuda JL et al. Tracking the response of natural killer T cells to a glycolipid antigen using CD1d tetramers. J. Exp. Med. 192, 741–754 (2000). [PubMed: 10974039]

26. Brossay L et al. CD1d-mediated recognition of an α-galactosylceramide by natural killer T cells is highly conserved through mammalian evolution. J. Exp. Med. 188, 1521–1528 (1998). [PubMed: 9782129]
27. Exley M et al. CD1d structure and regulation on human thymocytes, peripheral blood T cells, B cells and monocytes. Immunology 100, 37–47 (2000). [PubMed: 10809957]
28. Canchis PW et al. Tissue distribution of the non-polymorphic major histocompatibility complex class I-like molecule, CD1d. Immunology 80, 561–565 (1993). [PubMed: 7508419]
29. Tupin E, Kinjo Y & Kronenberg M The unique role of natural killer T cells in the response to microorganisms. Nat. Rev. Microbiol. 5, 405–417 (2007). [PubMed: 17487145]
30. van der Vliet HJ. et al. Circulating Vα24+Vβ11+NKT cell numbers are decreased in a wide variety of diseases that are characterized by autoreactive tissue damage. Clin. Immunol. 100, 144–148 (2001). [PubMed: 11465942]
31. Akbari O et al. Essential role of NKT cells producing IL-4 and IL-13 in the development of allergen-induced airway hyperreactivity. Nat. Med. 9, 582–588 (2003). [PubMed: 12669034]
32. Vivier E, Ugolini S, Blaise D, Chabannon C & Brossay L Targeting natural killer cells and natural killer T cells in cancer. Nat. Rev. Immunol. 12, 239–252 (2012). [PubMed: 22437937]
33. Kaneko Y et al. Augmentation of Vα14 NKT cell-mediated cytotoxicity by interleukin 4 in an autocrine mechanism resulting in the development of concanavalin A-induced hepatitis. J. Exp. Med. 191, 105–114 (2000). [PubMed: 10620609]
34. Wondimu Z, Santodomingo-Garzon T, Le T & Swain MG Protective role of interleukin-17 in murine NKT cell-driven acute experimental hepatitis. Am. J. Pathol. 177, 2334–2346 (2010). [PubMed: 20847291]
35. Kita H et al. Quantitation and phenotypic analysis of natural killer T cells in primary biliary cirrhosis using a human CD1d tetramer. Gastroenterology 123, 1031–1043 (2002). [PubMed: 12360465]
36. Durante-Mangoni E et al. Hepatic CD1d expression in hepatitis C virus infection and recognition by resident proinflammatory CD1d-reactive T cells. J. Immunol. 173, 2159–2166 (2004). [PubMed: 15265953]
37. Kakimi K, Guidotti LG, Koezuka Y, & Chisari FV Natural killer T cell activation inhibits hepatitis B virus replication in vivo. J. Exp. Med. 192, 921–930 (2000). [PubMed: 11015434]
38. Zeissig S et al. Hepatitis B virus-induced lipid alterations contribute to natural killer T cell-dependent protective immunity. Nat. Med. 18, 1060–1068 (2012). [PubMed: 22706385]
39. Mattner J et al. Liver autoimmunity triggered by microbial activation of natural killer T cells. Cell Host Microbe 3, 304–315 (2008). [PubMed: 18474357]
40. Boirivant M, Fuss IJ, Chu A & Strober W Oxazolone colitis: a murine model of T helper cell type 2 colitis treatable with antibodies to interleukin 4. J. Exp. Med. 188, 1929–1939 (1998). [PubMed: 9815270]
41. Nieuwenhuis EES et al. CD1d and CD1d-restricted iNKT-cells play a pivotal role in contact hypersensitivity. Exp. Dermatol. 14, 250–258 (2005). [PubMed: 15810882]
42. Heller F, Fuss IJ, Nieuwenhuis EE, Blumberg RS & Strober W Oxazolone colitis, a Th2 colitis model resembling ulcerative colitis, is mediated by IL-13-producing NK-T cells. Immunity 17, 629–638 (2002). [PubMed: 12433369]
43. Osman Y et al. Activation of hepatic NKT cells and subsequent liver injury following administration of alpha-galactosylceramide. Eur. J. Immunol. 30, 1919–1928 (2000). [PubMed: 10940881]
44. Barral DC & Brenner MB CD1 antigen presentation: how it works. Nat. Rev. Immunol. 7, 929–941 (2007). [PubMed: 18037897]
45. Im JS et al. Kinetics and cellular site of glycolipid loading control the outcome of natural killer T cell activation. Immunity 30, 888–898 (2009). [PubMed: 19538930]
46. Wal Yvande et al. Delineation ofa CD1d-restricted antigen presentation pathway associated with human and mouse intestinal epithelial cells. Gastroenterology 124, 1420–1431 (2003). [PubMed: 12730881]

47. Brigl M, Bry L, Kent SC, Gumperz JE & Brenner MB Mechanism of CD1d- restricted natural killer T cell activation during microbial infection. Nat. Immunol. 4, 1230–1237 (2003). [PubMed: 14578883]

48. Olszak T et al. Protective mucosal immunity mediated by epithelial CD1d and IL-10. Nature 509, 497–502 (2014). [PubMed: 24717441]

49. Sonoda K-H, Exley M, Snapper S, Balk SP & Stein-Streilein J Cd1-reactive natural killer T cells are required for development of systemic tolerance through an immune-privileged site. J. Exp. Med. 190, 1215–1225 (1999). [PubMed: 10544194]

50. Berntsen NL et al. Establishment of a surgical bile duct injection technique giving direct access to the bile ducts for studies of the murine biliary tree. Am. J. Physiol. Liver Physiol. 314, G349–G359 (2018).

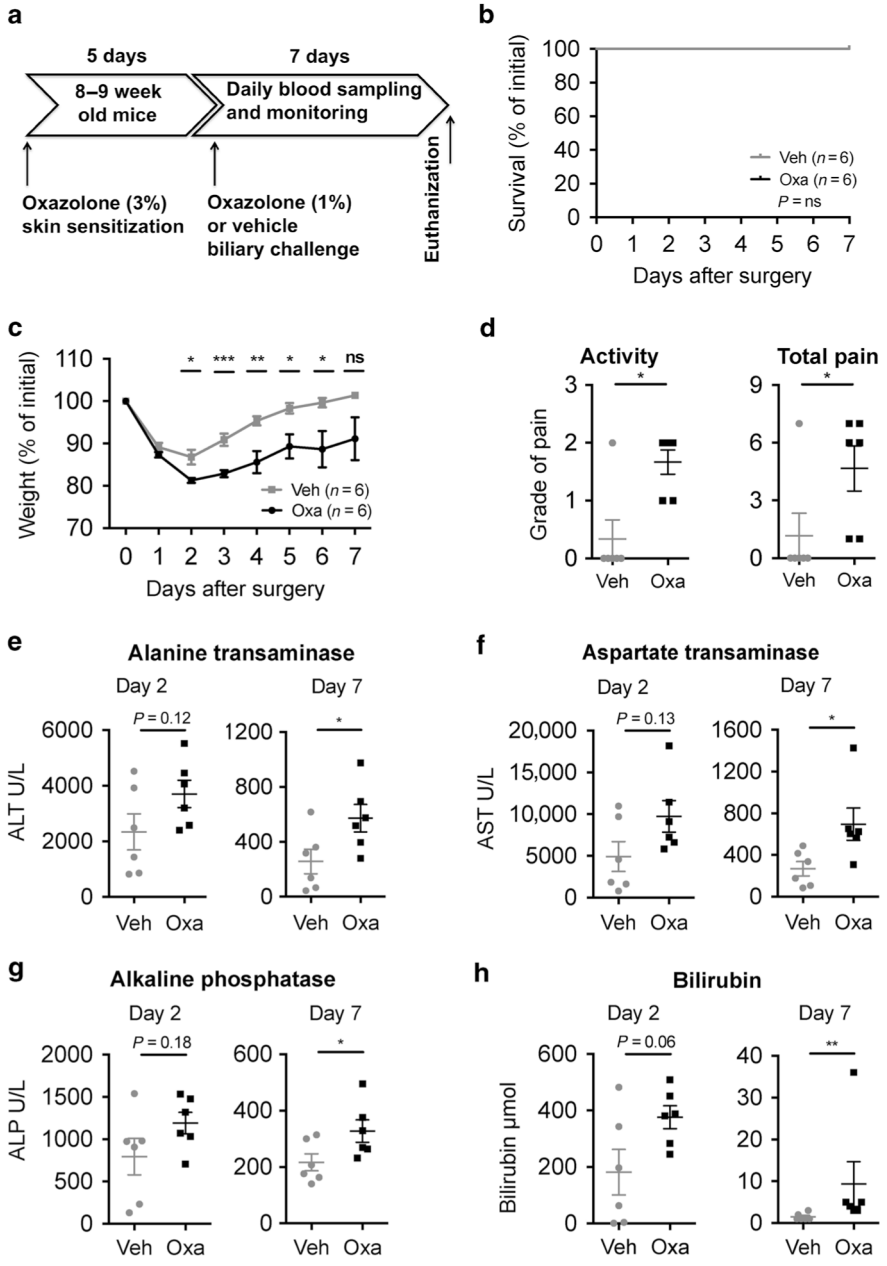

Fig. 1.

Biliary oxazolone challenge causes cholangitis. Timeline (**a**) demonstrating establishment of a novel cholangitis model with biliary oxazolone challenge 5 days after skin sensitization, and 7 days postoperative follow-up before killing. Survival (**b**) and weight (**c**) curves comparing biliary challenge of oxazolone ($n = 6$) to vehicle ($n = 6$) at indicated days. Evaluation of change in activity where the score indicates grade of pain as either absent (0), mild (1), moderate (2) or severe (3) and total pain with scoring on activity level/behavior (0–3), appearance (0–3) and clinical signs (0–3) (**d**) in indicated mice 2 days after surgery. Serum values of ALT (**e**) AST (**f**), ALP (**g**) and bilirubin (**h**) at days 2 and 7 after surgery in indicated mice. Each symbol represents a single mouse. Representative results from three

independent experiments are shown, presented as mean±SEM. Oxa oxazolone, Veh vehicle, ALT alanine transaminase, AST aspartate transaminase, ALP alkaline phosphatase, ns nonsignificant. *P <0.05, **P <0.01, ***P <0.001

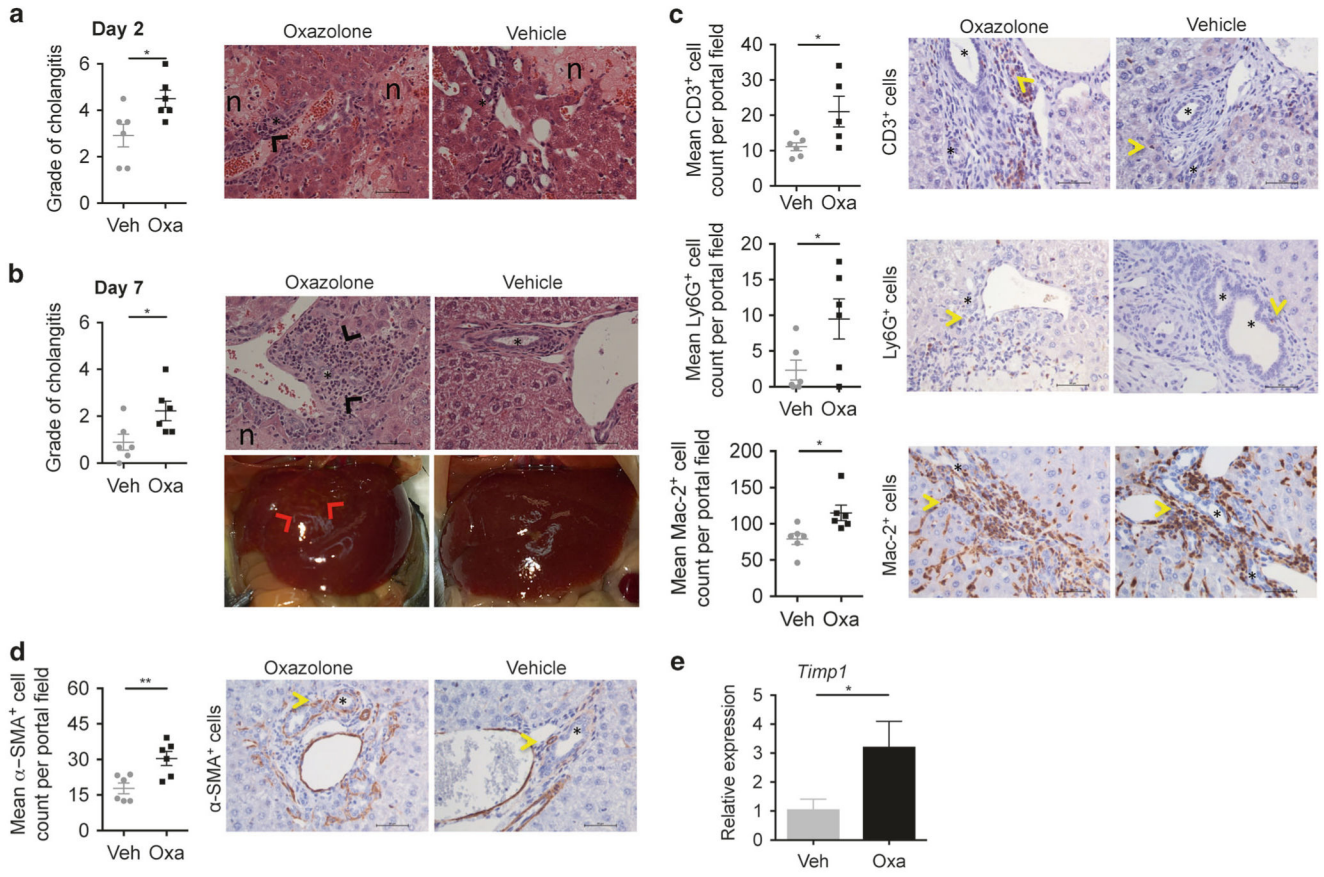

Fig. 2.

Oxazolone leads to inflammation of the portal area. Histologic evaluation of cholangitis with scoring on combined portal inflammation (0–3) and necrosis (0–3), where the score indicates degree of pathology as either absent (0), mild (1), moderate (2) or severe (3) and representative H&E staining of livers when comparing biliary injection of oxazolone with vehicle after 2 (**a**) and 7 (**b**) days, with additional demonstration of macroscopic liver appearance after 7 days (**b**). Immunohistochemical staining and figures showing mean CD3/Ly6G/Mac-2 (**c**) and α-SMA (**d**) positive cell count from six different high-power fields (40×) surrounding bile ducts of specified mice. CD3, Ly6G, Mac-2 and α-SMA are markers of T cells, neutrophils, macrophages and myofibroblasts, respectively. Bar graph showing relative expression of fibrosis marker gene *Timp1* (**e**) in livers of indicated mice ($n = 6$ in each group). Fold change in expression in each sample calculated as relative to the average expression in vehicle control mice. Each symbol represents a single mouse. Data from one representative experiment, presented as mean±SEM. Microscopic photos captured in 40× magnification, scale bars represent 50 μm (asterisks: bile ducts; black arrowheads: portal inflammation; red arrowheads: inflammatory changes; n: necrosis; yellow arrowheads: CD3-, Ly6G-, Mac-2- and α-SMA-positive cells.) H&E hematoxylin and eosin, Oxa oxazolone, Veh vehicle, Timp1 tissue inhibitor of metalloproteinases 1. $*P < 0.05$, $**P < 0.01$

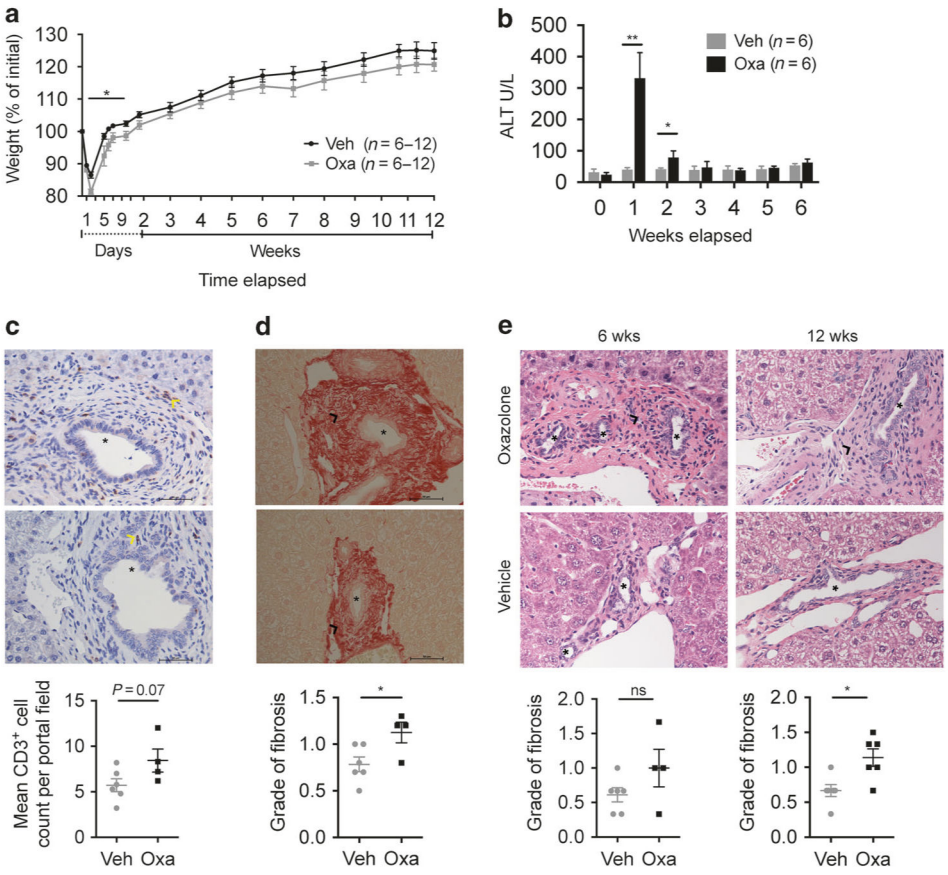

Fig. 3.

Long-term effects of oxazolone cholangitis. Weight curve (**a**) comparing biliary injection of oxazolone with vehicle over 6 ($n = 12$) or 12 ($n = 6$) weeks. Serum values of ALT (**b**) measured weekly and CD3-positive cells (T-cell marker, indicated by yellow arrowheads) around the bile ducts with a figure showing mean CD3-positive cell count from six different high-power fields (40×) surrounding bile ducts of indicated mice after 6 weeks (**c**). Sirius red staining (40×) after 6 weeks (**d**) and histologic evaluation of portal fibrosis where the score indicates degree of pathology as either absent (0), mild (1) or moderate (2) in indicated mice with representative H&E staining (40×) of livers after 6 and 12 weeks (**e**). Scale bars represent 50 μm (asterisks: bile ducts; black arrowheads: portal fibrosis; yellow arrowheads: CD3-positive cells). Each symbol represents a single mouse. Data from one representative experiment, except for the weight curve (**a**) where data were pooled for weeks 0–6 from two experiments with different time points for killing, presented as mean±SEM. Representative results from three independent experiments with 6-week follow-up are shown, while the experiment with 12-week time point was not repeated. H&E hematoxylin and eosin, Oxa oxazolone, Veh vehicle, ALT alanine transaminase, wks weeks, ns nonsignificant. *$P < 0.05$, **$P < 0.01$

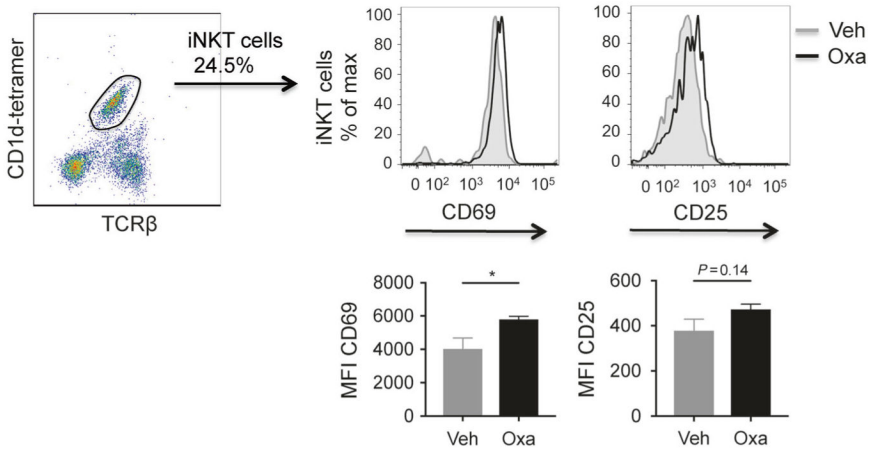

Fig. 4.

Activation of liver iNKT cells after intrabiliary oxazolone injection as measured by flow cytometry. Gating strategy of iNKT cells from representative samples of mononuclear cells isolated from the liver and expression of CD69 and CD25 2 days after injection of oxazolone or vehicle in the bile ducts. Gray tinted histograms represent vehicle and black lines represent oxazolone. Bar graphs show CD69 and CD25 expression measured by median fluorescence value in mice injected with oxazolone ($n = 4$) or vehicle ($n = 4$). Data from one representative experiment, presented as mean ± SEM. Oxa oxazolone, Veh vehicle, MFI median fluorescence intensity, iNKT invariant natural killer T. *$P < 0.05$

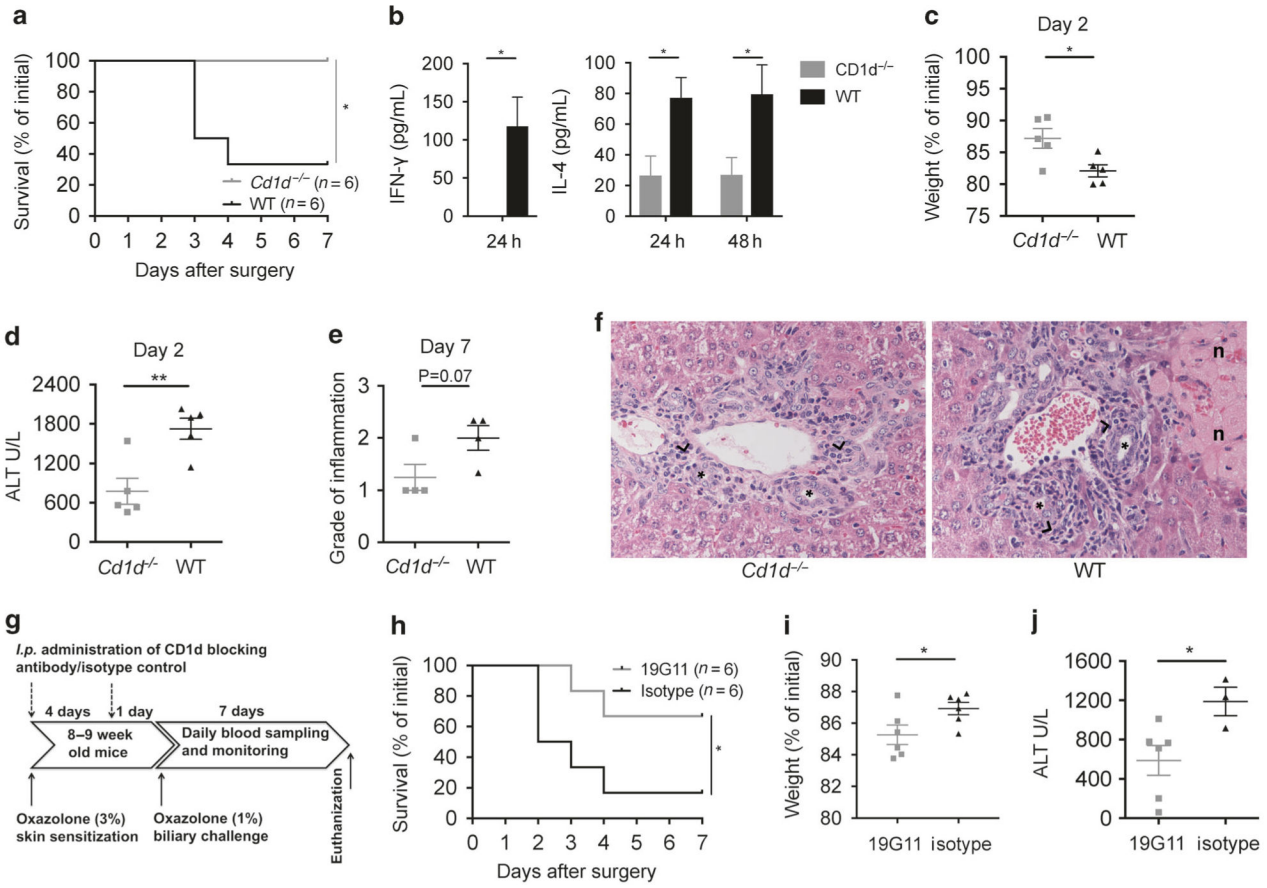

Fig. 5.

Oxazolone cholangitis is dependent upon CD1d and NKT cells. Survival curve (**a**) comparing *Cd1d*$^{-/-}$ and WT mice upon biliary oxazolone challenge. Bar graphs showing serum concentrations of IFN-γ and IL-4 at indicated time points after biliary oxazolone challenge in WT ($n = 5$) and *Cd1d*$^{-/-}$ ($n = 5$) mice (**b**). Weight loss (**c**), peak serum ALT levels (**d**) and histologic evaluation of portal inflammation (**e**) where the score indicates degree of pathology as either absent (0), mild (1), moderate (2) or severe (3) at the indicated days after biliary challenge with oxazolone in *Cd1d*$^{-/-}$ and WT mice. Representative H&E staining of livers (**f**) 7 days after biliary oxazolone challenge in the indicated mouse strains, captured in 40× magnification (asterisks: bile ducts; black arrowheads: portal inflammation; n: necrosis). Timeline (**g**) showing the oxazolone cholangitis model with biliary oxazolone challenge 5 days after skin sensitization and 7 days postoperative follow-up before killing, with additional i.p. injection of a CD1d-blocking antibody, 19G11 or isotype control at two time points: first at the time of skin sensitization and second the day before the surgery. Survival (**h**) of WT mice upon biliary oxazolone challenge and antibody blocking with either 19G11 or isotype control. Weight loss (**i**) at day 1 and peak serum ALT levels (**j**) at day 2 after oxazolone challenge in indicated mice. Each symbol represents a single mouse. Representative results from three independent experiments are shown, presented as mean ±SEM. ALT alanine transaminase, H&E hematoxylin and eosin, IFN interferon, IL interleukin, WT wild type. *$P < 0.05$, **$P < 0.01$